

Article

3D Printing of a Double Network Hydrogel with a Compression Strength and Elastic Modulus Greater than that of Cartilage

Feichen Yang, Vaibhav Tadepalli, and Benjamin J. Wiley

ACS Biomater. Sci. Eng., **Just Accepted Manuscript** • DOI: 10.1021/acsbmaterials.7b00094 • Publication Date (Web): 03 Apr 2017Downloaded from <http://pubs.acs.org> on April 3, 2017

Just Accepted

“Just Accepted” manuscripts have been peer-reviewed and accepted for publication. They are posted online prior to technical editing, formatting for publication and author proofing. The American Chemical Society provides “Just Accepted” as a free service to the research community to expedite the dissemination of scientific material as soon as possible after acceptance. “Just Accepted” manuscripts appear in full in PDF format accompanied by an HTML abstract. “Just Accepted” manuscripts have been fully peer reviewed, but should not be considered the official version of record. They are accessible to all readers and citable by the Digital Object Identifier (DOI®). “Just Accepted” is an optional service offered to authors. Therefore, the “Just Accepted” Web site may not include all articles that will be published in the journal. After a manuscript is technically edited and formatted, it will be removed from the “Just Accepted” Web site and published as an ASAP article. Note that technical editing may introduce minor changes to the manuscript text and/or graphics which could affect content, and all legal disclaimers and ethical guidelines that apply to the journal pertain. ACS cannot be held responsible for errors or consequences arising from the use of information contained in these “Just Accepted” manuscripts.

3D Printing of a Double Network Hydrogel with a Compression Strength and Elastic Modulus Greater than that of Cartilage

*Feichen Yang, Vaibhav Tadepalli, and Benjamin J. Wiley**

Department of Chemistry, Duke University, Durham, NC 27708, USA.

Email: Benjamin.wiley@duke.edu

Mailing address: Department of Chemistry, Duke University, 124 Science Drive, Box 90354, Durham, North Carolina 27708, United States.

KEYWORDS: tough hydrogel, double network hydrogel, 3D printing, tissue engineering.

ABSTRACT: This paper demonstrates a two-step method to 3D print double network hydrogels at room temperature with a low-cost (\$300) 3D printer. A first network precursor solution was made 3D printable via extrusion from a nozzle by adding a layered silicate to make it shear-thinning. After printing and UV-curing, objects were soaked in a second network precursor solution and UV-cured again to create interpenetrating networks of poly(2-acrylamido-2-methylpropanesulfonate) and polyacrylamide. By varying the ratio of polyacrylamide to cross-linker, the tradeoff between stiffness and maximum elongation of the gel can be tuned to yield a compression strength and elastic modulus of 61.9 and 0.44 MPa, respectively, values that are greater than those reported for bovine cartilage. The maximum compressive (93.5 MPa) and tensile (1.4 MPa) strengths of the gel are twice that of previous 3D printed gels, and the gel does

1
2
3 not deform after it is soaked in water. By 3D printing a synthetic meniscus from an X-ray
4
5 computed tomography image of an anatomical model, we demonstrate the potential to customize
6
7 hydrogel implants based on 3D images of a patient's anatomy.
8
9

10 11 **1. Introduction**

12
13
14 The meniscus, a network of tightly-woven collagen fibers, serves as a shock absorber for the
15
16 knee. A meniscal tear is among the most common knee injuries with more than 500,000 reported
17
18 in the United States annually.¹ Serious tears in the meniscus often do not heal and require
19
20 surgery to repair. For the most severe tears the entire meniscus is removed in a process known as
21
22 a meniscectomy.² Between 2005 and 2011, 387,000 meniscectomies were performed in the
23
24 United States.¹
25
26

27
28 If a patient who has previously lost a meniscus does begin to develop pain from early
29
30 degeneration in the same knee compartment, they may be a candidate for meniscal replacement
31
32 surgery.³ Currently, the only FDA approved synthetic meniscus replacement product is
33
34 NUSurface®.⁴ Though it provides mechanical support, its non-porous structure does not
35
36 stimulate tissue regeneration, which could lead to failure over time due to wear, fatigue, or an
37
38 adverse body response.^{5,6} Two other meniscal replacement solutions that have undergone clinical
39
40 trials, CMI® and Actifit®, do have the ability to stimulate tissue regeneration due to their porous
41
42 nature, but this tissue is not the fibrocartilage that makes up the meniscus.⁷⁻¹² In addition, CMI®
43
44 and Actifit® do not have the strength to serve as a total meniscus replacement, and therefore
45
46 have only been used as partial replacements in patients with some meniscus tissue remaining.¹¹
47
48
49
50
51

52 Double network (DN) hydrogels may offer an innovative alternative to a meniscectomy by
53
54 enabling the production of a customized synthetic meniscus. DN hydrogels are an extremely
55
56 strong family of hydrogels that are comprised of two non-covalently bonded, interpenetrating
57
58
59
60

1
2
3 polymer networks.¹³ It's been shown that, because of its unique porous and elastic structure, DN
4 hydrogels stimulate articular cartilage regeneration.¹⁴ As the meniscus acts as a buffer between
5 two pieces of bone, any replacement should be able to withstand significant compressive stress
6 with minimal distortion. A synthetic meniscus would ideally be custom-made for the patient and
7 rapidly produced at a relatively low cost, suggesting that 3D printing is a promising method for
8 the production of synthetic menisci. Researchers have developed various approaches to 3D print
9 hydrogel materials that are suitable for tissue engineering applications, including the use of
10 liquid extrusion based 3D printing,¹⁵⁻¹⁹ two-photon polymerization,²⁰ dynamic optical projection
11 stereolithography²¹ and fused deposition modeling followed by cell culturing.^{22,23} However,
12 current 3D printable hydrogels do not meet the compression strength (14-59 MPa) required for
13 replacing a human meniscus.
14
15
16
17
18
19
20
21
22
23
24
25
26
27
28

29 One approach to obtaining a 3D printable, tough hydrogel consists of using ionic crosslinking
30 to reinforce the gel. Zhao et al. 3D printed a hybrid hydrogel made from a poly(ethylene glycol)
31 diacrylate (PEGDA) network and alginate crosslinked by Ca^{2+} . This gel had a maximum fracture
32 energy of 1500 J m^{-2} .¹⁶ Spinks et al. used extrusion printing to produce a polyacrylamide gel
33 reinforced by an alginate- Ca^{2+} network; this gel had a toughness of 260 kJ m^{-3} .²⁴ Unfortunately,
34 these 3D printable hydrogels disintegrate upon exposure to water because the calcium required
35 for reinforcing the gel leaches out, making them unsuitable for *in situ* and *in vivo* applications.
36
37
38
39
40
41
42
43
44
45

46 Another approach to 3D print a tough hydrogel is to print a gel with a temperature-dependent
47 viscosity. Cong et al. used a 3D printer with a heated cartridge to print a polyacrylamide
48 hydrogel reinforced with both agar and ionically crosslinked alginate at $45\text{-}60 \text{ }^\circ\text{C}$.¹⁹ Although
49 they achieved a toughness of 3860 kJ m^{-3} , using a heated syringe increases the complexity of the
50
51
52
53
54
55
56
57
58
59
60

1
2
3 printing process. Other strategies of reinforcing 3D printed hydrogels involve 3D printing a
4 hydrogel-plastic composite²⁵ or encapsulating hydrogel in epoxy resin.²⁶
5
6
7

8 In this paper, we report the development of a shear-thinning ink that enables the printing of a
9 DN hydrogel at room temperature. The concentration of Laponite, a layered silicate, and the
10 molecular precursors of the first network were tuned to enable the ink to easily extrude through a
11 fine nozzle, but have sufficient viscosity after printing to retain the shape of a 3D printed object
12 with a height up to 35 mm. Printing was performed with an easily modified \$300 3D printer.
13 After printing, objects were UV-cured, soaked in the precursor solution of the second network,
14 and UV-cured again to form a DN hydrogel. The mechanical properties of the DN hydrogels can
15 be tuned to have a compression strength approaching 100 MPa, double that of any previous 3D
16 printed hydrogel. Objects printed with this gel retain their shape and mechanical integrity after
17 soaking in water.
18
19
20
21
22
23
24
25
26
27
28
29
30

31 **2. Materials and Methods**

32 **2.1 Preparation of Hydrogel Precursor Solutions.** Sodium 2-acrylamido-2-
33 methylpropanesulfonate (AMPS), acrylamide, N,N'-methylenebis(acrylamide) (MBAA) and
34 Irgacure 2959 (I2959) were purchased from Sigma Aldrich. Laponite RDS was donated by BYK
35 additive.
36
37
38
39
40
41
42

43 To make the 3D printable gel precursor, 1.0 g Laponite RDS, 50 mg I2959 and 60 mg MBAA
44 were dissolved in 8.1 g water. The solution was allowed to stir overnight to homogenize, and 1.9
45 g of a 50 wt% AMPS solution was slowly added. The final concentrations of the components in
46 the ink were 10 w/v% Laponite RDS, 0.40 M AMPS, 40 mM MBAA and 22mM I2959. The first
47 network precursor was cured with a variable intensity UV transilluminator (VWR, 26XV).
48
49
50
51
52
53
54
55
56
57
58
59
60

1
2
3 The second network precursor was made by dissolving 14 wt% acrylamide (2.0 M), 0.01 wt%
4 MBAA (0.64 mM) and 0.05 wt% (22 mM) I2959 in 10 g water. After UV curing, the first
5 network gel was soaked in the second network precursor for 24 hours. The fully soaked gel was
6 subsequently cured again with a variable intensity UV transilluminator (VWR, 26XV) in N₂
7 atmosphere. For the precursors with 4.0 and 6.0 M acrylamide, the concentration of I2959 was
8 kept the same at 22 mM, and the molar ratio of acrylamide to MBAA was kept the same at
9 ~3125.
10
11
12
13
14
15
16
17
18

19
20 **2.2 3D printing of DN Hydrogel.** To 3D print the DN hydrogel, a Reprap Prusa i3 3D printer
21 was modified by replacing the thermoplastic filament extruder with a 3D printed syringe pump.
22 The 3D model of the syringe pump is available for downloading at:
23 <http://www.thingiverse.com/thing:1923150>. A 5 mL syringe and a 21-gauge needle was used for
24 extrusion. The first network precursor was loaded into the syringe and distributed to certain
25 positions in 3D space according to a gcode file. After 3D printing, the printed object was cured
26 with a variable intensity UV transilluminator (VWR, 26XV) for 10 minutes to 3 hours,
27 depending on the size of the hydrogel. Following the first UV curing step, the object was soaked
28 in the second network precursor for 24h, then cured again in a N₂ atmosphere for 30 minutes. To
29 test the maximum height of 3D printed objects with this method, a 3D model of a 10 mm × 10
30 mm × 100 mm pillar was created and 3D printed. As the pillar increased in height during printing,
31 the weight of the pillar caused it to compress. Compression of the pillar caused the distance
32 between the needle and the pillar to increase until eventually (at a height of 35 mm) no additional
33 gel could be extruded from the needle onto the pillar.
34
35
36
37
38
39
40
41
42
43
44
45
46
47
48
49
50
51

52
53 **2.3 Mechanical Characterization.** Dogbone-shaped samples were 3D printed according to
54 ASTM D412 for tensile tests on a micro-strain analyzer (TA Instrument, RSA III). The exact
55
56
57
58
59
60

1
2
3 dimensions of samples were measured with a caliper before testing. Tensile tests were performed
4
5 at a shear speed of 0.1 mm s^{-1} . The stress-strain curve between 0-10% strain was used to
6
7 calculate the Young's modulus. Compression tests were performed on a materials testing
8
9 machine (Instron, model 1321) on a shear speed of 0.1 mm s^{-1} . Cylindrical samples with a
10
11 diameter of 10 mm and a height of 8 mm were 3D printed with the procedure described above.
12
13 The exact sizes of samples were measured with a caliper before testing. The stiffness
14
15 measurements were performed on a rheometer (TA Instrument, AR-G2). The stiffness data were
16
17 extracted by linear regression of the stress-strain curve in the range of 0-10% strain. Viscosities
18
19 of aqueous solutions of AMPS and Laponite RDS were measured on a rheometer (TA Instrument,
20
21 AR-G2) with a 2° cone and plate geometry. Yield strain was determined with the 0.2% offset
22
23 method. A line was drawn parallel to the linear part of the stress-strain curve, intersecting the
24
25 "strain" axis at 0.2%. The yield strain was determined as the intersection of this line to the stress-
26
27 strain curve.
28
29
30
31
32

34 **3. Results and Discussion**

36 **3.1 3D Printing of Double Network Hydrogel**

37
38 Figure 1 shows an overview of the steps for 3D printing a DN hydrogel. A video (Movie S1)
39
40 of the gel printing is available in the supporting information. The process starts by 3D printing a
41
42 suspension containing 10% w/v Laponite RDS, 0.40 M sodium 2-acrylamido-2-
43
44 methylpropanesulfonate (AMPS), 40 mM N,N'-methylenebis(acrylamide) (MBAA), and 22 mM
45
46 Irgacure 2959. Laponite RDS is a layered silicate rheology modifier that was added to control the
47
48 viscosity of the ink, AMPS is the monomer for the first network hydrogel, MBAA is a cross-
49
50 linker, and Irgacure 2959 is a photoinitiator for UV curing. After printing, the object was UV
51
52 cured to form a stiff and brittle hydrogel consisting of poly(2-acrylamido-2-
53
54
55
56
57
58
59
60

1
2
3 methylpropanesulfonate), which is abbreviated as PAMPS. To improve its mechanical strength, a
4
5 second interpenetrating network was created by soaking the first hydrogel network in an
6
7 acrylamide solution, causing it to swell by 20%-750%. The swelling ratio is affected by the
8
9 amount of MBAA in the first network, which in turn affects the stiffness of the gel. After
10
11 soaking overnight, the fully swollen hydrogel was cured with UV light, forming a tough DN
12
13 hydrogel consisting of an interpenetrating network of PAMPS and polyacrylamide. We note that
14
15 both of these gels have been demonstrated to be biocompatible after the removal of acrylamide
16
17 monomer by dialysis.^{14,27,28}
18
19
20
21
22
23
24
25
26
27
28
29
30
31
32
33
34
35
36
37
38
39
40
41
42
43
44
45
46
47
48
49
50
51
52
53
54
55
56
57
58
59
60

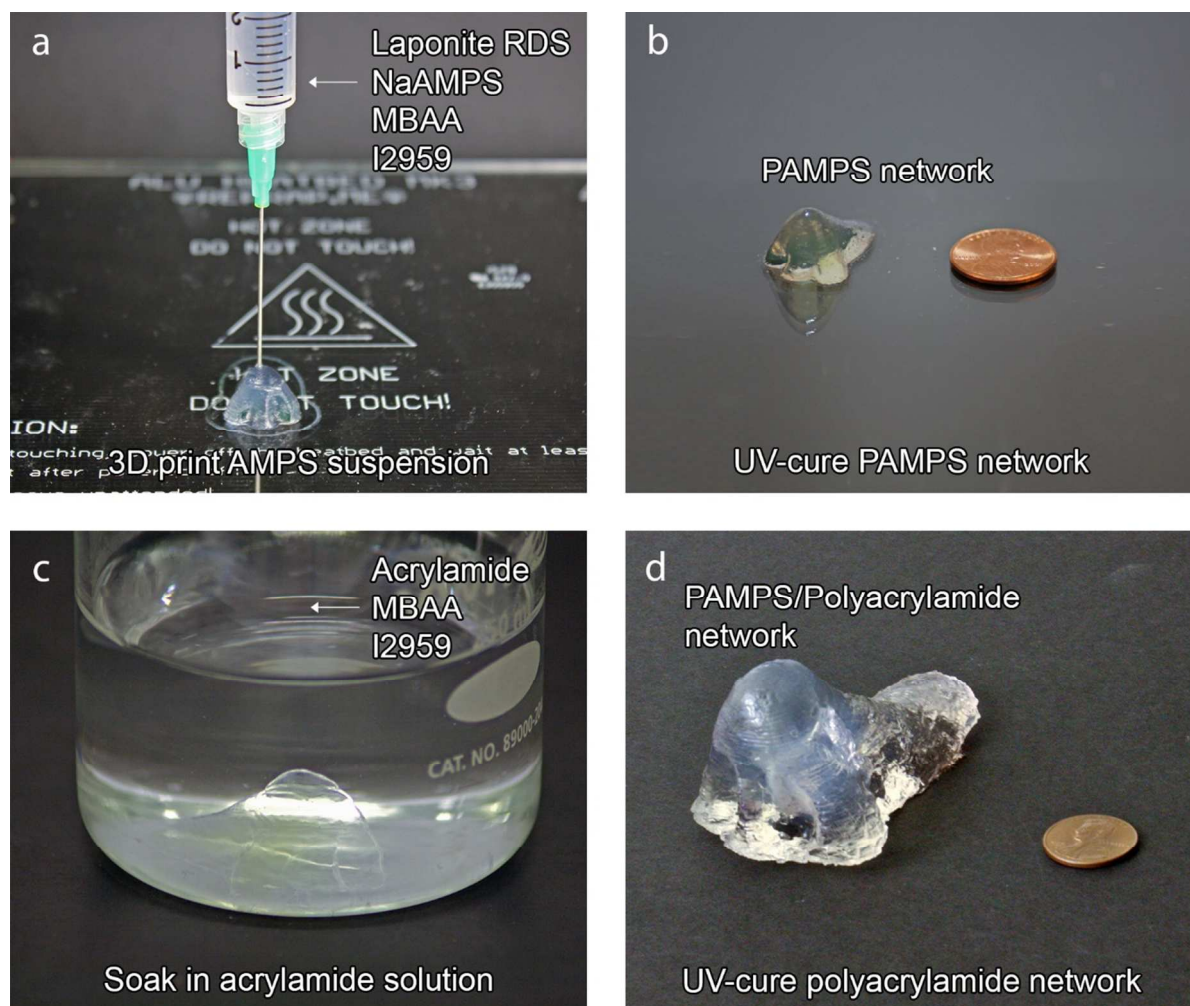


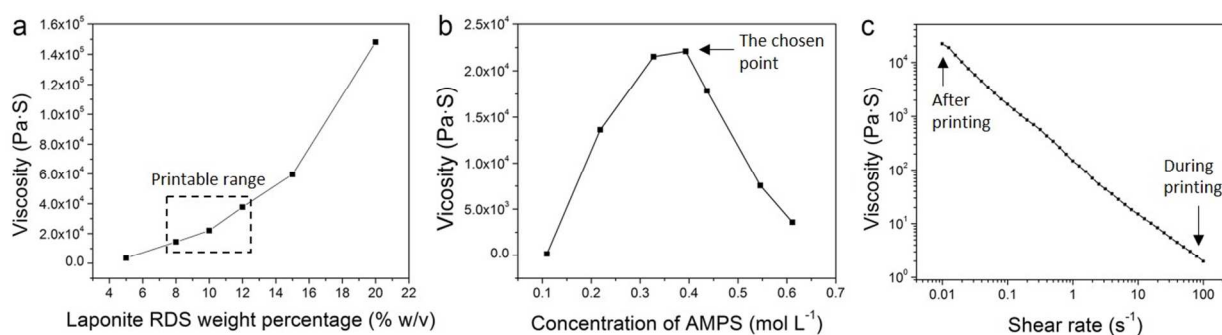
Figure 1. Steps for 3D printing a DN hydrogel. (a) 3D print the AMPS suspension; (b) UV-cure to obtain the PAMPS network; (c) Soak the PAMPS network in an acrylamide solution; (d) UV-cure to obtain a PAMPS/polyacrylamide double network.

3.2 Optimizing the Viscosity of AMPS Solution for Printability

The 3D printed DN hydrogel described here was inspired by the PAMPS-polyacrylamide double network first reported by Gong et al.¹³ However, in its original formulation this gel was not 3D printable. For 3D printing, the gel precursor should have a low viscosity during extrusion so it can flow, and a high viscosity once extruded so it can retain its shape. Since the viscosity of the first network precursor is too low to maintain a 3D structure after printing, the addition of a

1
2
3 rheology modifier is necessary to enable the gel precursor to be 3D printed. The pH of solutions
4 containing 2-acrylamido-2-methylpropane sulfonic acid (used in the original work by Gong et
5 al.) are generally too low for thickening by most rheology modifiers such as layered silicates,
6 alginate or cellulose. Therefore, we replaced this acid with sodium 2-acrylamido-2-
7 methylpropane sulfonate. Laponite RDS was then added to create a shear-thinning gel.²⁹ We note
8 that Laponite RDS is a biocompatible material that is safe for food contact applications, and thus
9 should not compromise the biocompatibility of the PAMPS-polyacrylamide hydrogel.²⁹
10
11
12
13
14
15
16
17
18
19

20 Figure 2a shows the effect of adding Laponite RDS to a solution of 0.40 M AMPS. Without
21 Laponite, the viscosity of the AMPS solution is approximately equal to that of water (3.0 Pa·s).
22 Addition of Laponite increases the viscosity from 3.5 kPa·s at 5 w/v% to 148.1 kPa·s at 20
23 w/v%. By 3D printing these different viscosities, we found that a viscosity of 14.48-37.72 kPa·s
24 (8-12 w/v% Laponite) was sufficient to enable an object to retain its shape after extrusion
25 without the frequent clogging of the nozzle that occurs if the viscosity is too high. The
26 intermediate concentration of 10 w/v % Laponite RDS was chosen for all the following printing
27 experiments.
28
29
30
31
32
33
34
35
36
37
38
39
40
41
42
43
44
45
46
47
48
49



50
51 **Figure 2.** (a) Viscosity of aqueous solutions containing 0.40 M AMPS and different amounts of
52 Laponite RDS; (b) Viscosity of aqueous solutions containing 10 w/v% Laponite RDS with
53 different amounts of AMPS; (c) The viscosity of the 3D printable gel precursor as a function of
54 shear rate.
55
56
57
58
59
60

1
2
3 We also found that the concentration of the AMPS monomer has a strong effect on the
4 viscosity of the 3D printable gel precursor. Changing the concentration of this precursor changes
5 the ionic strength of the solution, which is known to affect the viscosity of a Laponite
6 suspension.²⁹ We found that the viscosity was at a maximum with a concentration of 0.40 M
7 AMPS. Although a higher concentration of AMPS would result in a gel with a higher strength,
8 suspensions with higher concentrations of AMPS didn't retain their shape after printing due to
9 their lower viscosity. Therefore, for all the following experiments we used a concentration of
10 0.40 M AMPS in the 3D printed gel precursor.
11
12
13
14
15
16
17
18
19
20
21

22 Figure 2c demonstrates the shear-thinning properties of a solution containing 10 w/v%
23 Laponite RDS and 0.40 M AMPS. When the suspension is extruded at a speed of 5.0 mm s⁻¹, its
24 shear rate can be calculated with the following formula, wherein $\dot{\gamma}$ is the shear rate, v is the linear
25 flow rate of fluid in the nozzle and d is the inside diameter of the needle):³⁰
26
27
28
29
30
31

$$\dot{\gamma} = \frac{8v}{d} = \frac{8 \times 5.0 \text{ mm s}^{-1}}{0.514 \text{ mm}} = 78 \text{ s}^{-1}$$

32
33
34
35
36 At this shear rate, the low viscosity of the suspension allows it to be easily extruded. As soon
37 as the gel precursor leaves the nozzle, it reverts to the high viscosity state and the lack of fluid
38 flow enables the printing of the liquid in a wide variety of shapes, with heights up to ~35 mm.
39
40
41
42
43

44 3.3 3D Printing of DN Hydrogel

45
46 The rheological properties of the gel precursor ink allow it to be printed with most liquid
47 extrusion-based 3D printers, such as those that use a syringe or air pressure to dispense a liquid
48 solution. For this paper we used a modified Prusa i3 3D printer available for about \$300 (see
49 Figure S1). We replaced the original polymer extruder with a syringe-based extruder consisting
50 of 3D printed parts and lead screw stepper motor.³¹ Conventional 3D modeling software
51
52
53
54
55
56
57
58
59
60

(Tinkercad, Autodesk 123D) was used to design the objects, and these shapes were converted to gcode files for 3D printing using Cura as the slicing program.

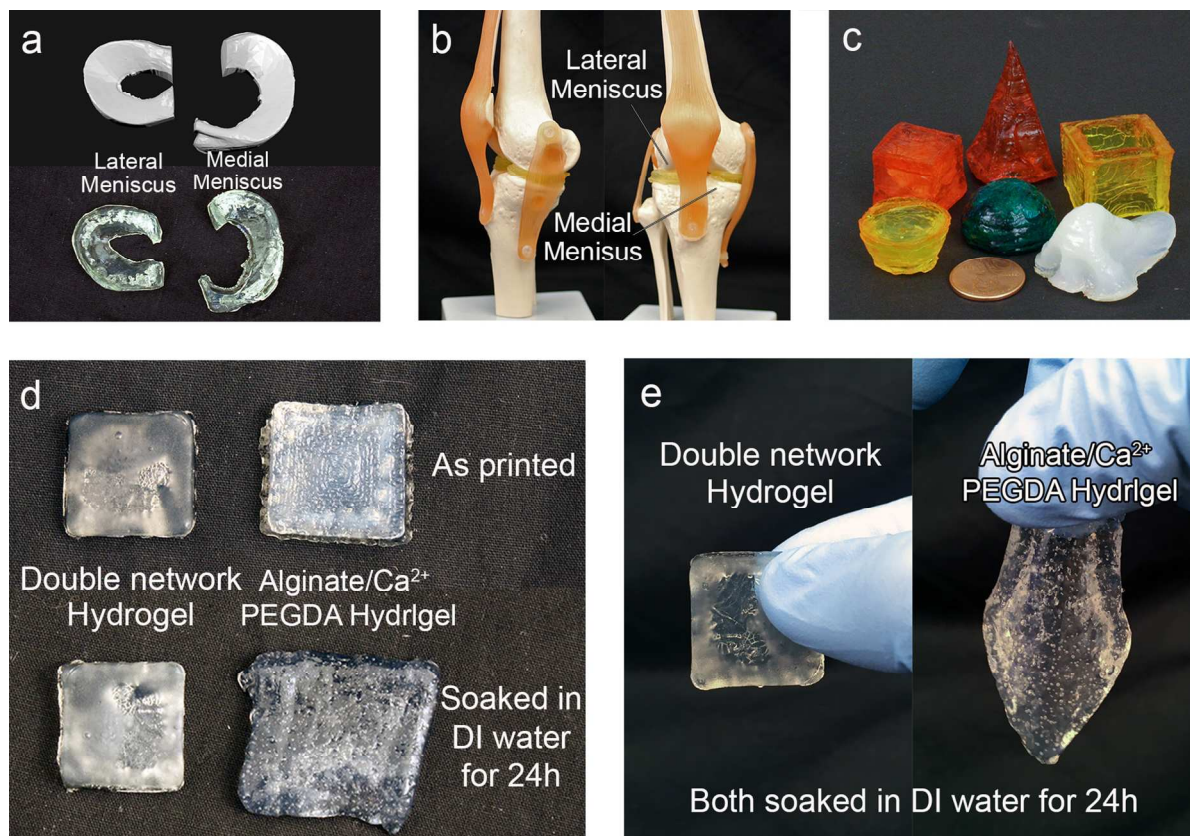


Figure 3. (a) Top: 3D model of a pair of menisci; Bottom: 3D printed DN hydrogel menisci; The 3D model was obtained by scanning an anatomical model of a human knee with a High Resolution X-ray Computed Tomography Scanner (MicroCT); (b) The 3D printed menisci in the knee model; (c) Front row: a reverse cone (yellow), a hemisphere (green) and a human nose scan (off-white); Back row: a cube (red), a sharp pyramid (red) and a square tube (yellow). Food coloring was added to make the originally transparent gels more visible; (d) The 3D printed hydrogel from this work (left) retains its shape after soaking in DI water for 24 hours while a 3D printed PEGDA+alginate/ Ca^{2+} semi-interpenetrating hydrogel swells; (e) A piece of 3D printed double network hydrogel retains its shape when held, but the 3D printed PEGDA hydrogel was deformed by gravity.

1
2
3 Figure 3 demonstrates the 3D printing of menisci with the DN hydrogel. In Figure 3a, a 3D
4 model of a pair of menisci was obtained by scanning an anatomical model of a human knee with
5 X-ray computed tomography. A pair of artificial menisci was then 3D printed based on that 3D
6 model, and put back into the same knee model as a replacement. Since it was obtained from the
7 original menisci shape, the 3D printed meniscus fits the model joint perfectly with no
8 modifications after printing. We imagine a similar workflow could potentially be used for real
9 patients, in which 3D images of their menisci served as the starting point for creating a
10 replacement. In contrast, partial synthetic meniscus replacements such as CMI® and Actifit® are
11 not customized for each patient, but are instead trimmed from a standard shape by hand using a
12 scalpel.^{32,33} The whole meniscus replacement product NUSurface® also comes in seven standard
13 sizes that are not customizable, and finding the right size can involve some trial and error during
14 surgery.^{4,34,35}

15
16
17
18
19
20
21
22
23
24
25
26
27
28
29
30
31
32 Figure 3c shows a series of objects to demonstrate that a variety of geometries can be printed
33 with the shear-thinning gel precursor. The thin pyramid demonstrates printing of objects with
34 high vertical aspect ratios. The reverse cone demonstrates printing of an overhang. The human
35 nose demonstrates the ability to print complex anatomical structures that combine the need to
36 print a high vertical aspect ratio and overhangs. The minimum spacing between printed lines
37 (Figure S2) that could be achieved with a needle diameter of 500 μm without the lines touching
38 was 750 μm , demonstrating that minimal spreading occurs after printing of the ink. This
39 resolution can likely be improved by using a needle with a smaller diameter.

40
41
42
43
44
45
46
47
48
49
50
51
52
53
54
55
56
57
58
59
60
After soaking in the second network precursor, the printed first network swells and exhibits a
volume increase of 20%- 750%. This swelling is isotropic, and the degree of swelling must be
taken into account when designing an object with a desired size. Swelling decreases the

1
2
3 resolution and minimum feature size that can be printed for a given needle diameter. The degree
4
5 of swelling depends largely on the concentration of MBAA in the first network; a higher
6
7 concentration of MBAA in the first network leads to less swelling because of the increase in
8
9 stiffness with higher concentrations of MBAA. Thus, swelling can be minimized at high MBAA
10
11 concentrations.
12
13

14
15 In order to be used *in vivo*, a gel-based meniscus should not lose its shape and strength after
16
17 prolonged soaking in water. In Figure 3d, we compare the shape of the DN gel to a previously
18
19 reported PEGDA+alginate/Ca²⁺ semi-interpenetrating hydrogel.¹⁶ There is no observable change
20
21 in the shape of the DN gel after immersion in DI water for 24 hours, but the PEGDA-based gel
22
23 clearly deforms as the Ca²⁺ leaches into solution. In Figure 3e, both the DN gel and the
24
25 PEGDA+alginate/Ca²⁺ gel was soaked in DI water for 24 hours, then suspended by hand. While
26
27 the DN hydrogel retained its stiffness after the 24-hour soak, the PEGDA+alginate/Ca²⁺ gel was
28
29 immediately deformed by gravity.
30
31
32
33
34
35
36
37
38
39
40
41
42
43
44
45
46
47
48
49
50
51
52
53
54
55
56
57
58
59
60

3.4 Tensile Characteristics of DN Hydrogel

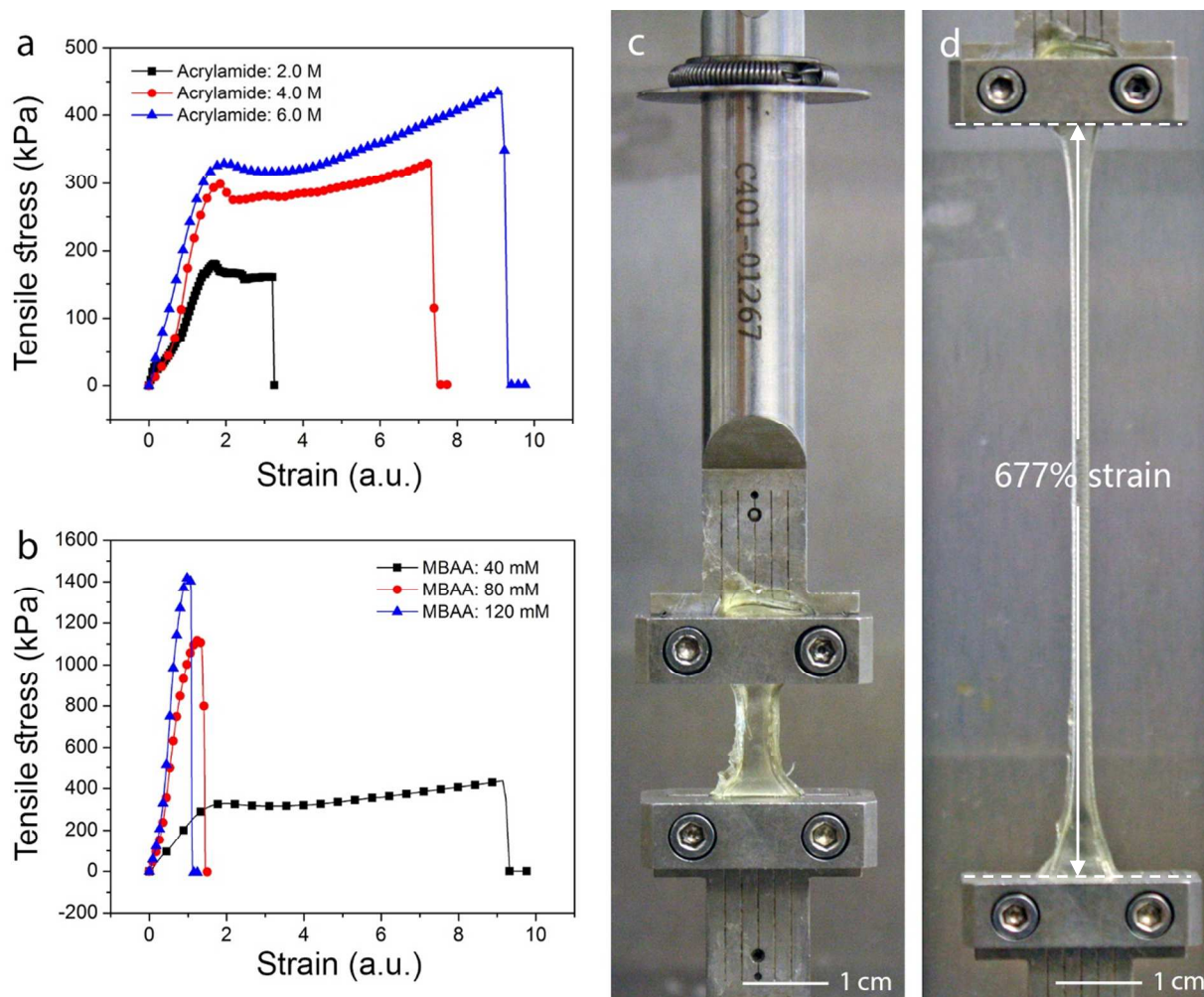


Figure 4. (a) Tensile stress-strain curve of samples with 40 mM MBAA in the first network and different concentrations of acrylamide in the second network; (b) Tensile stress-strain curve of samples with different concentrations of MBAA in the first network and 6.0 M acrylamide in the second network; (c)-(d) a dogbone with 40 mM MBAA and 6.0 M acrylamide before and after stretching to 677% strain.

The mechanical properties of the 3D-printable DN hydrogel could be tuned by changing the concentration of crosslinker, MBAA, in the first network, or the concentration of acrylamide in the second network while keeping the molar ratio of acrylamide to MBAA in the second network

1
2
3 constant at 3125:1. Figure 4a shows that increasing the concentration of acrylamide in the second
4 network from 2.0 to 6.0 M increases the maximum elongation strain from 322% to 923%, with a
5 concurrent increase in toughness from 404.1 kJ m⁻³ to 3024 kJ m⁻³. This toughness is similar to
6 the best result previously reported (3860 kJ m⁻³) that relied on an alginate-Ca²⁺ network.¹⁹ The
7 yield strain of all samples shown in Figure 4a & b is listed in Table S1.
8
9

10
11
12
13
14
15 Although increasing the acrylamide concentration leads to excellent toughness, the elastic
16 modulus and tensile strength may not be sufficient for some applications. Therefore, we also
17 explored the effect of the crosslinker, MBAA, on the stiffness of the PAMPS-polyacrylamide
18 DN hydrogel. Figure 4b demonstrates that the elastic modulus of the DN hydrogel with 120 mM
19 MBAA is 1060 kPa, which is 449% greater than that of the DN hydrogel with 40 mM MBAA. Both
20 of these gels were made with 6.0 M of acrylamide in the second network. More MBAA in the
21 first network also decreases the maximum elongation from 923% to 112%. Thus, tuning the
22 MBAA crosslinker concentration allows one to tune the gel to exhibit a desired tradeoff between
23 stiffness and maximum elongation. The increase in stiffness that results from increasing the
24 amount of MBAA also affects the swelling behavior of the first network during immersion in the
25 second network precursor solution. Hydrogels with 40 mM MBAA exhibited a volume increase
26 of 650% during the soaking step, but the swelling ratio of hydrogels with 120 mM MBAA was
27 less than 120%.
28
29
30
31
32
33
34
35
36
37
38
39
40
41
42
43
44

45
46 Previous research has shown that the toughness of the DN hydrogel is related to local yielding
47 effects.³⁶ When stretched over the yield strain, the brittle first network fractures and dissipates
48 energy. This phenomenon can be seen in a comparison of the stress-strain curves that show the
49 first and second cycle of tensile testing (Figure S3). After the first cycle, it is thought that the
50 fracture of the first network creates a less stiff, sliding-ring hydrogel with different stress-strain
51
52
53
54
55
56
57
58
59
60

1
2
3 characteristics.³⁷ These results show that the 3D printed DN hydrogel reported here has similar
4
5 mechanical properties as previously reported PAMPS-polyacrylamide DN hydrogels, despite the
6
7 modifications made to make it 3D printable.
8
9

10 **3.5 Compression characteristics of DN Hydrogel**

11
12 Compression tests were performed on the 3D printed gels to determine their suitability for the
13
14 replacement of meniscus cartilage. Figure 5a & b shows that a DN hydrogel with 40 mM MBAA
15
16 in the first network and 2.0 M acrylamide in the second network has the biggest compression
17
18 fracture strength of 93.5 MPa. Increasing the concentration of acrylamide increases the stiffness
19
20 of the gel in the low-strain region, while leading to a lower maximum stress in the high-strain
21
22 region. The compression strength of the DN hydrogel decreased from 93.5 MPa to 10.5 MPa
23
24 when the acrylamide concentration was increased from 2.0 to 6.0 M. Higher compression
25
26 strengths can be obtained without a loss of ductility by increasing the concentration of MBAA in
27
28 the first network. When the MBAA concentration was increased from 40 to 120 mM in the first
29
30 network and the acrylamide concentration was kept at 6.0 M, the compression strength increased
31
32 from 10.5 to 61.9 MPa, while retaining a maximum strain of 99%. If the MBAA concentration
33
34 was further increased to 140 mM, the gel became more brittle and fractured at a strain of 75%,
35
36 leading to a decreased compression strength of 5.05 MPa.
37
38
39
40
41
42
43
44
45
46
47
48
49
50
51
52
53
54
55
56
57
58
59
60

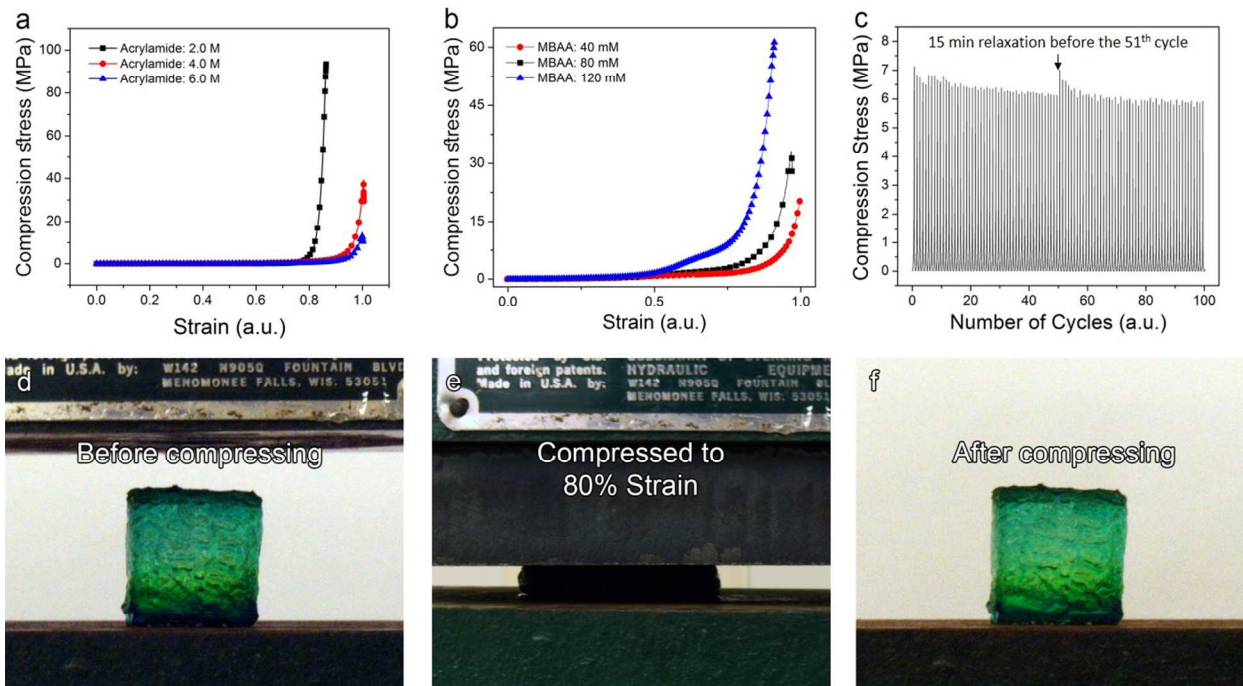


Figure 5. (a) Compression stress-strain curves of DN hydrogels made with 40 mM MBAA and varying concentrations of acrylamide; (b) Compression stress-strain curves of DN hydrogels made with 6.0 M of acrylamide and varying amounts of MBAA; (c) Compression stress for a DN hydrogel with 120 mM MBAA and 6.0 M acrylamide at a strain of 75% strain over 100 cycles. The gel was relaxed at cycle 50 for 15 minutes; (d)-(f) a piece of cubic DN hydrogel before, during, and after being compressed to 80% strain.

In Figure 5d-5f, a 3D printed cube of DN gel with 40 mM MBAA in the first network and 6.0 M acrylamide in the second network was compressed to 80% strain, then released, showing no visible sign of plastic deformation after compression. To further test the fatigue resistance of the DN hydrogel material, a cylindrical DN hydrogel sample was compressed to a strain of 75% with a shear rate of 1 mm s^{-1} , the position was held for 1 second, and the gel was released back to its original height at a speed of 1 mm s^{-1} . After the first 50 cycles, the maximum stress in each cycle decreased from 7.12 MPa to 6.14 MPa. In order to determine if the softening effect was

1
2
3 reversible, the sample was rested for 15 minutes before being compressed for another 50 cycles.
4
5 As shown in Figure 5c, the maximum stress recovered to a value of 7.01 MPa after relaxation,
6
7 which indicates that the loss of strength of the DN hydrogel is temporary. After the 60th cycle,
8
9 the stress plateaued at 5.87 MPa, showing only some fluctuations. The softening is likely due to
10
11 the fact that the gel requires several minutes before it goes to back to its original height. After the
12
13 first compression cycle, the total height of the gel is slightly smaller than it was originally, but
14
15 the original height was still used for the strain calculation. This results in the gel being
16
17 compressed to a strain several percent smaller than 75%, leading to a smaller stress.
18
19
20
21

22 **3.6 Comparison of 3D Printed Tough Hydrogels and Bovine Cartilage**

23
24 Table 1 compares the various mechanical properties of bovine articular cartilage, previously
25
26 reported 3D printed hydrogels, and several optimized gels in this work. By tuning the formula of
27
28 the 3D printed DN hydrogel, the mechanical properties can be tuned to surpass those of most
29
30 other gels. The 3D printed gel with 120 mM MBAA in the first network and 6.0 M acrylamide in
31
32 the second network was found to be the best potential meniscus replacement (See Figure S4 and
33
34 Figure 5b) due to its excellent stiffness (0.44 MPa compared to 0.31 MPa of bovine femur
35
36 cartilage) and compression strength (61.9 MPa compared to 14-59 MPa of bovine cartilage).
37
38 Although a further increase of the MBAA concentration in the first network increases the
39
40 stiffness of the 3D printed gels, it causes the gel to be brittle and ultimately lowers the
41
42 compression strength.^{38,39}
43
44
45
46
47
48
49
50
51
52
53
54
55
56
57
58
59
60

Table 1. Mechanical properties of bovine cartilage and 3D printed hydrogels.

	Compression Strength (MPa)	Tensile Strength (MPa)	Elastic Modulus (MPa)		Toughness (kJ m ⁻³)
			Tensile	Compression	
Bovine Cartilage ^{38,40,41}	14-59	0.53-9	10.1-28.3	0.31	-
Polyacrylamide-Alginate+Ca ²⁺ ²⁴	-	0.17	0.066	-	260
Agar-Polycrylamide-Alginate+Ca ²⁺ ^{19,42}	40	0.781	0.810	-	3860
40 mM MBAA, 2.0 M Acrylamide	93.5	0.160	0.069	0.051	401.4
40 mM MBAA, 6.0 M Acrylamide	17.9	0.437	0.167	0.11	3024
120 mM MBAA, 6.0 M Acrylamide	61.9	1.417	1.016	0.44	1060

4. Conclusions

In conclusion, this paper introduces a method to 3D print double network hydrogels that have a compression strength, tensile strength, and elastic modulus greater than any previous 3D printed gels. Tuning the ratio of cross-linker in the first network to the acrylamide monomer in the second network allowed for the formulation of a gel with a compression strength and stiffness greater than that of bovine cartilage. In addition, the DN hydrogels could be printed at room temperature with a modified \$300 3D printer, and exhibited no deformation after soaking in water for 24 hours. This new gel presents an opportunity to customize hydrogel implants based on X-ray computed tomography images of a patient's own anatomy. Future work may examine the relationship between the mechanical properties of this printed gel and its potential to stimulate cartilage tissue growth.

1
2
3 ASSOCIATED CONTENT
45 **Supporting Information.**
6

7
8 The following files are available free of charge.
9

10 Figure S1-S4; (PDF)

11
12 Table S1; (PDF)

13
14
15 Movie S1; (AVI)
16
17

18 **Funding Sources**
19

20
21 This work was supported in part by start-up funds from Duke University, NSF Grant No.
22 ECCS-1344745 and an NSF CAREER award (DMR-1253534).
23
24
25
26
27

28 ACKNOWLEDGMENT
29

30
31 We acknowledge the assistance of Dr. Richard Glisson (Duke University Medical Center,
32
33 Duke University) for the compression testing experiments.
34
35

36 REFERENCES
37

38
39 (1) Abrams, G. D.; Frank, R. M.; Gupta, A. K.; Harris, J. D.; McCormick, F. M.; Cole, B. J.
40
41 Trends in meniscus repair and meniscectomy in the United States, 2005-2011. *Am. J. Sport. Med.*
42
43 **2013**, *41*, 2333-2339.
44
45

46
47 (2) DEHAVEN, K. E. Decision-making factors in the treatment of meniscus lesions. *Clin.*
48
49 *Orthop. Relat. R.* **1990**, *252*, 49-54.
50
51

52
53 (3) McDermott, I. Meniscal tears, repairs and replacement: their relevance to osteoarthritis of
54
55 the knee. *Brit. J. Sport. Med.* **2011**, *45*, 292-297.
56
57
58
59
60

1
2
3 (4) NUsurface® Meniscus Implant. [https://activeimplants.com/products/nusurface-meniscus-](https://activeimplants.com/products/nusurface-meniscus-implant/)
4 implant/ (accessed Dec 20 2016).
5
6

7
8 (5) Hollister, S. J. Porous scaffold design for tissue engineering. *Nat. Mater.* **2005**, *4*, 518-524.
9

10
11 (6) Vrancken, A. C. T.; Buma, P.; van Tienen, T. G. Synthetic meniscus replacement: a review.
12
13 *Int. Ortho.* **2013**, *37*, 291-299.
14
15

16
17 (7) What is Actifit®-Actifit. <http://actifit.info/what-is-actifit/> (accessed Dec 20 2016).
18
19

20
21 (8) Stone, K. R.; Rodkey, W. G.; Webber, R.; McKinney, L.; Steadman, J. R. Meniscal
22 regeneration with copolymeric collagen scaffolds In vitro and in vivo studies evaluated
23 clinically, histologically, and biochemically. *Am. J. Sport. Med.* **1992**, *20*, 104-111.
24
25
26

27
28 (9) Maher, S. A.; Rodeo, S. A.; Doty, S. B.; Brophy, R.; Potter, H.; Foo, L.-F.; Rosenblatt, L.;
29 Deng, X.-H.; Turner, A. S.; Wright, T. M. Evaluation of a porous polyurethane scaffold in a
30 partial meniscal defect ovine model. *Arthroscopy.* **2010**, *26*, 1510-1519.
31
32
33

34
35 (10) Collagen Meniscus Implant. <http://www.ivysportsmed.com/en/collagen-meniscus-implant>
36 (accessed Dec 20 2016).
37
38

39
40 (11) Welsing, R. T.; van Tienen, T. G.; Ramrattan, N.; Heijkants, R.; Schouten, A. J.; Veth, R.
41 P.; Buma, P. Effect on Tissue Differentiation and Articular Cartilage Degradation of a Polymer
42 Meniscus Implant A 2-Year Follow-up Study in Dogs. *Am. J. Sports. Med.* **2008**, *36*, 1978-1989.
43
44
45
46

47
48 (12) Spencer, S.; Saithna, A.; Carmont, M.; Dhillon, M.; Thompson, P.; Spalding, T. Meniscal
49 scaffolds: early experience and review of the literature. *The Knee* **2012**, *19*, 760-765.
50
51
52
53
54
55
56
57
58
59
60

1
2
3 (13) Gong, J. P.; Katsuyama, Y.; Kurokawa, T.; Osada, Y. Double-network hydrogels with
4 extremely high mechanical strength. *Adv. Mater.* **2003**, *15*, 1155-1158.
5
6
7

8
9 (14) Yasuda, K.; Kitamura, N.; Gong, J. P.; Arakaki, K.; Kwon, H. J.; Onodera, S.; Chen, Y.
10 M.; Kurokawa, T.; Kanaya, F.; Ohmiya, Y. A Novel Double - Network Hydrogel Induces
11 Spontaneous Articular Cartilage Regeneration in vivo in a Large Osteochondral Defect.
12
13
14
15
16
17
18
19
20
21
22
23
24
25
26
27
28
29
30
31
32
33
34
35
36
37
38
39
40
41
42
43
44
45
46
47
48
49
50
51
52
53
54
55
56
57
58
59
60

(15) Kolesky, D. B.; Truby, R. L.; Gladman, A. S.; Busbee, T. A.; Homan, K. A.; Lewis, J. A.
3D Bioprinting of Vascularized, Heterogeneous Cell-Laden Tissue Constructs. *Adv. Mater.*
2014, *26*, 3124-3130.

(16) Hong, S.; Sycks, D.; Chan, H. F.; Lin, S.; Lopez, G. P.; Guilak, F.; Leong, K. W.; Zhao,
X. 3D printing of highly stretchable and tough hydrogels into complex, cellularized structures.
Adv. Mater. **2015**, *27*, 4035-4040.

(17) Bertassoni, L. E.; Cardoso, J. C.; Manoharan, V.; Cristino, A. L.; Bhise, N. S.; Araujo, W.
A.; Zorlutuna, P.; Vrana, N. E.; Ghaemmaghami, A. M.; Dokmeci, M. R. Direct-write
bioprinting of cell-laden methacrylated gelatin hydrogels. *Biofabrication* **2014**, *6*, 024105.

(18) Hinton, T. J.; Jallerat, Q.; Palchesko, R. N.; Park, J. H.; Grodzicki, M. S.; Shue, H.-J.;
Ramadan, M. H.; Hudson, A. R.; Feinberg, A. W. Three-dimensional printing of complex
biological structures by freeform reversible embedding of suspended hydrogels. *Sci. Adv.* **2015**,
1, e1500758.

(19) Wei, J.; Wang, J.; Su, S.; Wang, S.; Qiu, J.; Zhang, Z.; Christopher, G.; Ning, F.; Cong,
W. 3D printing of an extremely tough hydrogel. *Rsc Adv.* **2015**, *5*, 81324-81329.

1
2
3 (20) Hahn, M. S.; Miller, J. S.; West, J. L. Three-dimensional biochemical and biomechanical
4 patterning of hydrogels for guiding cell behavior. *Adv. Mater.* **2006**, *18*, 2679-2684.
5
6

7
8
9 (21) Zhang, A. P.; Qu, X.; Soman, P.; Hribar, K. C.; Lee, J. W.; Chen, S.; He, S. Rapid
10 Fabrication of Complex 3D Extracellular Microenvironments by Dynamic Optical Projection
11 Stereolithography. *Adv. Mater.* **2012**, *24*, 4266-4270.
12
13
14

15
16
17 (22) Kang, H.-W.; Lee, S. J.; Ko, I. K.; Kengla, C.; Yoo, J. J.; Atala, A. A 3D bioprinting
18 system to produce human-scale tissue constructs with structural integrity. *Nat. Biotechnol.* **2016**,
19
20
21
22
23
24
25
26
27
28
29
30
31
32
33
34
35
36
37
38
39
40
41
42
43
44
45

46 (23) Jakus, A. E.; Rutz, A. L.; Jordan, S. W.; Kannan, A.; Mitchell, S. M.; Yun, C.; Koube, K.
47 D.; Yoo, S. C.; Whiteley, H. E.; Richter, C.-P. Hyperelastic “bone”: A highly versatile, growth
48 factor-free, osteoregenerative, scalable, and surgically friendly biomaterial. *Sci. Transl. Med.*
49
50
51
52
53
54
55
56
57
58
59
60

61 (24) Bakarich, S. E.; Beirne, S.; Wallace, G. G.; Spinks, G. M. Extrusion printing of ionic-
62 covalent entanglement hydrogels with high toughness. *J. Mat. Chem. B* **2013**, *1*, 4939-4946.
63
64
65
66
67
68
69
70
71
72
73
74
75
76
77
78
79
80
81
82
83
84
85
86
87
88
89
90
91
92
93
94
95
96
97
98
99
100

99 (25) Zhao, X. Multi-scale multi-mechanism design of tough hydrogels: building dissipation
100 into stretchy networks. *Soft Matter* **2014**, *10*, 672-687.

101 (26) Bakarich, S. E.; Gorkin III, R.; in het Panhuis, M.; Spinks, G. M. Three-dimensional
102 printing fiber reinforced hydrogel composites. *ACS Appl. Mater. Inter.* **2014**, *6*, 15998-16006.
103
104
105
106
107
108
109
110
111
112
113
114
115
116
117
118
119
120
121
122
123
124
125
126
127
128
129
130
131
132
133
134
135
136
137
138
139
140
141
142
143
144
145
146
147
148
149
150
151
152
153
154
155
156
157
158
159
160

159 (27) Barry, R. A.; Shepherd, R. F.; Hanson, J. N.; Nuzzo, R. G.; Wiltzius, P.; Lewis, J. A.
160 Direct-Write Assembly of 3D Hydrogel Scaffolds for Guided Cell Growth. *Adv. Mater.* **2009**,
161
162
163
164
165
166
167
168
169
170
171
172
173
174
175
176
177
178
179
180
181
182
183
184
185
186
187
188
189
190
191
192
193
194
195
196
197
198
199
200

1
2
3 (28) Narita, T.; Ohtakeyama, R.; Matsukata, M.; Gong, J.; Osada, Y. Kinetic study of cell
4 disruption by ionic polymers with varied charge density. *Colloid Polym. Sci.* **2001**, *279*, 178-183.
5
6

7
8
9 (29) Laponite RDS Data sheet. [http://www.additives-](http://www.additives-downloads.de/output/ag_download.aspx?file=PB Laponite RDS_EN.pdf)
10 [downloads.de/output/ag_download.aspx?file=PB Laponite RDS_EN.pdf](http://www.additives-downloads.de/output/ag_download.aspx?file=PB Laponite RDS_EN.pdf) (accessed Sep 5 2015).
11
12

13
14 (30) Darby, R.: *Chemical Engineering Fluid Mechanics, Revised and Expanded*; Taylor &
15 Francis, **2001**; p64.
16
17

18
19
20 (31) Syringe pump. <http://www.thingiverse.com/thing:1923150> (accessed Nov 28 2016).
21
22

23 (32) CMI Surgery. [http://www.ivysportsmed.com/en/collagen-meniscus-implant/receiving-](http://www.ivysportsmed.com/en/collagen-meniscus-implant/receiving-cmi/cmi-surgery)
24 [cmi/cmi-surgery](http://www.ivysportsmed.com/en/collagen-meniscus-implant/receiving-cmi/cmi-surgery) (accessed Dec 22 2016).
25
26

27
28 (33) Actifit® procedure-Actifit. <http://actifit.info/patient-centre/actifit-procedure/> (accessed
29 Dec 22 2016).
30
31

32
33 (34) Farr, J.; Gomoll, A.: *Cartilage Restoration: Practical Clinical Applications*; 1 ed.;
34 Springer-Verlag New York, **2014**; pp. 237.
35
36

37
38 (35) Parker, D: *Management of Knee Osteoarthritis in the Younger, Active Patient*; Springer
39 Heideberg New York, **2016**; p151-152.
40
41

42
43 (36) Gong, J. P. Why are double network hydrogels so tough? *Soft Matter* **2010**, *6*, 2583-2590.
44
45

46
47 (37) Yasuda, K.; Gong, J. P.; Katsuyama, Y.; Nakayama, A.; Tanabe, Y.; Kondo, E.; Ueno,
48 M.; Osada, Y. Biomechanical properties of high-toughness double network hydrogels.
49 *Biomaterials* **2005**, *26*, 4468-4475.
50
51
52
53
54
55
56
57
58
59
60

1
2
3 (38) Schinagl, R. M.; Gurskis, D.; Chen, A. C.; Sah, R. L. Depth-dependent confined
4 compression modulus of full-thickness bovine articular cartilage. *J. Orthop. Res.* **1997**, *15*, 499-
5 506.
6
7
8

9
10
11 (39) Korhonen, R.; Laasanen, M.; Töyräs, J.; Rieppo, J.; Hirvonen, J.; Helminen, H.; Jurvelin,
12 J. Comparison of the equilibrium response of articular cartilage in unconfined compression,
13 confined compression and indentation. *J. Biomech.* **2002**, *35*, 903-909.
14
15
16

17
18
19 (40) Kerin, A.; Wisnom, M.; Adams, M. The compressive strength of articular cartilage. *P. I.*
20 *Mech. Eng. H.* **1998**, *212*, 273-280.
21
22
23

24
25 (41) Williamson, A. K.; Chen, A. C.; Masuda, K.; Thonar, E. J.; Sah, R. L. Tensile mechanical
26 properties of bovine articular cartilage: variations with growth and relationships to collagen
27 network components. *J. Orthop. Res.* **2003**, *21*, 872-880.
28
29
30

31
32
33 (42) Chen, Q.; Zhu, L.; Zhao, C.; Wang, Q.; Zheng, J. A Robust, One-Pot Synthesis of Highly
34 Mechanical and Recoverable Double Network Hydrogels Using Thermoreversible Sol - Gel
35 Polysaccharide. *Adv. Mater.* **2013**, *25*, 4171-4176.
36
37
38
39
40
41
42
43
44
45
46
47
48
49
50
51
52
53
54
55
56
57
58
59
60

1
2
3 Table of Contents graphic:
4
5
6

7
8
9
10
11
12
13
14
15
16
17
18
19
20
21
22
23
24
25
26
27
28
29
30
31
32
33
34
35
36
37
38
39
40
41
42
43
44
45
46
47
48
49
50
51
52
53
54
55
56
57
58
59
60

3D Printing of a Double Network Hydrogel with Cartilage-Like Mechanical Properties

*Feichen Yang, Vaibhav Tadepalli, and Benjamin J. Wiley**

